Oxidation Protection of High-Temperature Oxidation-Resistant Coatings

Subjects: Materials Science, Ceramics

Contributor: Yingyi Zhang

Molybdenum and its alloys, with high melting points, excellent corrosion resistance and high temperature creep resistance, are a vital high-temperature structural material. However, the poor oxidation resistance at high temperatures is a major barrier to their application.

molybdenum alloys coating oxidation behavior microstructure high-temperature

1. Introduction

Molybdenum and molybdenum-based alloys have a high melting point (2620 °C), good high-temperature mechanical properties and high conductivity and thermal conductivity, and are widely used in high-temperature structures [1][2][3][4][5][6]. However, the alloys have a poor oxidation resistance, and the “Pesting oxidation” at 400–800 °C and oxidation decomposition above 1000 °C are the main factors that limit their application [7][8][9][10]. At present, the alloying and surface-coating technology are the main methods to increase the oxidation resistance of the basal materials [11][12]. The types of molybdenum alloys and the various surface coating technologies of Mo and its alloys are shown in **Figure 1** [13][14][15][16]. It can been seen that the Ti, Zr, W, Re, Si, B, Hf, C and rare earth oxides are often added to pure Mo as beneficial elements to prepare molybdenum alloys. However, the result of alloying is not satisfactory when considering the mechanical properties and high-temperature oxidation resistance of the alloys [17][18]. For example, adding a certain amount Ti element to the alloy can enhance its strength, but it will further accelerate the oxidation of the alloy [19]. Mo–Si–B alloys have satisfactory high temperature oxidation resistance, but their fracture toughness is poor. Mo–Ti–Si–B alloys are considered as a promising ultra-high temperature material. However, their oxidation resistance and mechanical properties need to be further studied [20].

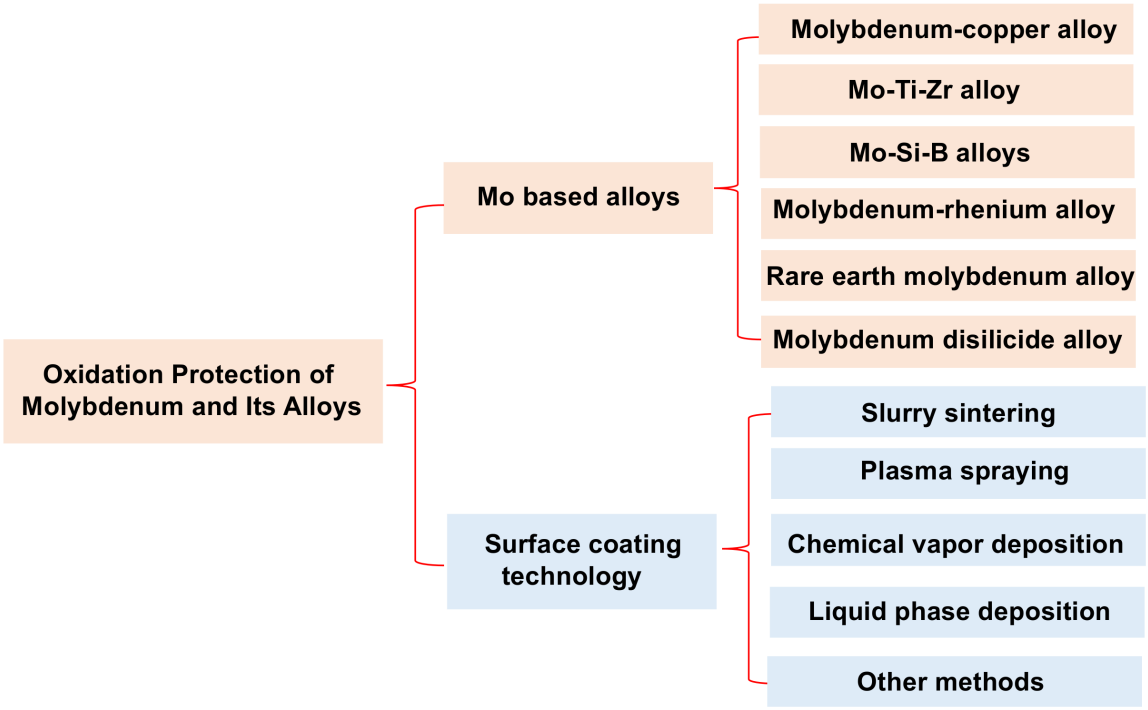

Figure 1. Overview of Mo alloy types and Mo and its alloy surface-coating technology.

2. Microstructure and Oxidation Behavior of Coatings

2.1. Coatings Prepared by Slurry Sintering (SS)

2.1.1. Microstructure and Growth Mechanism of SS Coatings

The slurry sintering (SS) method mixes alloy or silicide powder with binder in a certain proportion and then dissolves it in organic solvent to obtain the mixture. The mixture was evenly coated on the surface of the substrate, and then heated for a certain time in vacuum or Ar atmosphere, so that the substrate and mixture could be fully combined to form a coating on the surface [21][22].

2.1.2. Oxidation Behavior and Mechanism of SS Coatings

It is observed that an oxide layer forms on the surface of SS coatings after oxidation, which is mainly composed of SiO_2, TiO_2, Mo_5Si_3, etc. Compared with the original coating, the thickness of the oxidized coating increases significantly, which is due to the volume of the coating expanding and the interface migration caused by the inter-diffusion reaction. However, the thickness of the $MoSi_2$ layer decreases significantly due to the growth of the oxide film and the migration of the interface layer. By contrast, the interdiffusion between the coating and the substrate becomes more sufficient with the increase of exposure time, resulting in a significant increase in the thickness of the interface layer dominated by Mo_5Si_3 [23][24][25][26].

2.2. Coatings Prepared by Plasma-Spraying Technique

2.2.1. Microstructure and Growth Mechanism of Plasma-Spraying Coatings

The plasma-spraying technique is one of the most widely used coating preparation in thermal-spraying technology. Its principle is heating and ionizing a certain gas (N_2, H_2, Ar, He or their mixture) by an electric arc. The generated high-energy plasma arc can heat powdery materials to molten or semi-molten state and spray them onto the substrate surface at high speed to form a coating [27][28][29]. Among them, the air plasma spraying technique (APS), plasma-transferred arc (PTA) and spark plasma sintering (SPS) are widely used in the surface oxidation protection of Mo and its alloys.

2.2.2. Oxidation Behavior and Mechanism of Plasma-Spraying Coatings

It should be noted that except for Mo_2BC coating, the mass of the other coatings increases compared with that before oxidation. This is mainly due to the strong affinity force between C and oxygen. During oxidation, the volatilization rate of CO is greater than the formation rate of B_2O_3, resulting in the reduction of the overall quality of the coating.

2.3. Coatings Prepared by Chemical Vapor Deposition (CVD) Technology

2.3.1. Microstructure and Growth Mechanism of CVD Coatings

The principle behind chemical vapor deposition (CVD) technology is the process of using gaseous substances reacting with a solid substrate to generate solid deposits [30][31]. The process conditions and mechanical properties of the oxidation-resistant coatings prepared on molybdenum by the CVD technique as shown in **Table 1** [32][33][34][35][36].

Table 1. Summary of process, composition and properties of CVD coatings on Mo surface.

Substrate	Composition of Gas Mixture	Process Conditions			Composition and Thickness of Coatings (μm)		Bond Strength (MPa)	Hardness (GPa)	Surface Grain Size (μm)	Refs.
		Gas Flow Rate ($ml \cdot min^{-1}$)	Deposition Temperature (°C)	Deposition Time (h)	Outerlayer	Interface Layer				
Mo	$SiCl_4$, H_2	$SiCl_4$: 50.00 H_2: 100.00	620.00	3.00	SiO_2 (3.00)	$MoSi_2$ (5.00)	-	-	15.00	[32]
	NH_3, $SiCl_4$, H_2	NH_3: 100.00 H_2: 990.00 $SiCl_4$: 10.00	1100.00	NH_3: 2.00 $SiCl_4$: 5.00	$MoSi_2$, Si_3N_4 (72.00)	Mo_2N (5.00)	-	-	3.00 × 10^{-1}	[33]

Substrate	Composition of Gas Mixture	Process Conditions			Composition and Thickness of Coatings (μm)		Bond Strength (MPa)	Hardness (GPa)	Surface Grain Size (μm)	Refs.
		Gas Flow Rate ($ml \cdot min^{-1}$)	Deposition Temperature (°C)	Deposition Time (h)	Outerlayer	Interface Layer				
	BCl_3, $TiCl_4$, H_2	BCl_3: 195.00 $TiCl_4$: 130.00 H_2: 635.00	1000.00	2.00	TiB_2 (13.00)	-	7.00	28.00	2.00	[34]
	WCl_2, H_2	-	1800.00	2.00	W (160.00)	-	-	-	20.00	[35]
	CH_4, $SiCl_4$, H_2	CH_4, H_2:200.00 $SiCl_4$: 10.00 H_2: 990.00	1200.00, 1100.00	CH_4: 65.00 $SiCl_4$: 10.00	SiC, $MoSi_2$ (60.00)	MO_2C (25.00)	-	-	3.00×10^{-1}	[36]

2. Khlyu… …ntact with water during the formation of molybdenum oxide. Curr. Appl. Phys. 2020, 20, 1396–1403.
3. Kong, H.; Kwon, H.S.; Kim, H.; Jeen, G.S.; Lee, J.; Lee, J.; Heo, Y.S.; Cho, J.; Jeen, H. Reductive-annealing-induced changes in Mo valence states on the surfaces of MoO3 single crystals and their high temperature transport. Curr. Appl. Phys. 2019, 19, 1379–1382.
4. Bahamonde, O.H.; Wu, C.Z.; Lodge, S.M.; Bao, J.M.; Rodrigues, D.F. Oxidation state of Mo affects dissolution and visible-light photocatalytic activity of MoO3 nanostructures. J. Catal. 2020, 381, 508–519.
5. Smolik, G.R.; Petti, D.A.; Schuetz, S.T. Oxidation and volatilization of TZM alloy in air. J. Nucl. Mater. 2000, 283-287, 1458–1462.
6. Majumdar, S.; Kapoor, R.; Raveendra, S.; Sinha, H.; Samajdar, I.; Bhargava, P.; Chakravartty, J.K.; Sharma, I.G.; Suri, A.K. A study of hot deformation behavior and microstructural characterization of Mo–TZM alloy. J. Nucl. Mater. 2009, 385, 545–551.

2.3.2. Oxidation Behavior and Mechanism of CVD Coatings

Table 2 shows the microstructure evolution and mass gain of CVD coatings before and after oxidation under different conditions. Obviously, researchers mainly reported the oxidation of the coating at low temperature (500 °C to 1000 °C), and the oxidized coatings mainly consist of an oxide layer, intermediate layer and interface layer [32][33][34][35][36][37].

Table 2. Microstructure evolution and mass gain of CVD coatings on molybdenum before and after oxidation.

Substrate	Composition and Thickness of Coatings (μm)		Exposure	Comments	Composition and Thickness of Oxidized Coatings (μm)		Mass Gain ($mg \cdot cm^{-2}$)	Refs.
	Outer Layer	Interface Layer			Oxide Layer	Intermediate Layer		
Mo	SiO_2 (3.00)	$MoSi_2$ (5.00)	1000 °C, 3.00 h	-	SiO_2, MoO_3	$MoSi_2$-Mo_5Si_3	12.00	[32]
	$MoSi_2$-Si_3N_4 (72.00)	Mo_2N (5.00)	500 °C, 1492.00 h	1.00 h cycles	Si_2ON_2, SiO_2, $MoO_3Mo_4O_{11}$, Mo_9O_{26}, (3.00)	$MoSi_2$-Si_3N_4 (100.00)	5.00×10^{-1}	[33]
	TiB_2 (13.00)	-	900 °C, 6.00 h	-	TiO_2, B_2O_3	-	8.00×10^{-2}	[34]

1. … …ms. Mater. Sci. Eng. A 2021, 799, 139–891.

Substrate	Composition and Thickness of Coatings (μm)		Exposure	Comments	Composition and Thickness of Oxidized Coatings (μm)		Mass Gain ($mg \cdot cm^{-2}$)	Refs.
	Outer Layer	Interface Layer			Oxide Layer	Intermediate Layer		
	TiB_2 (13.00)	-	450 °C, 5.00 h	-	TiO_2, B_2O_3	-	3.00×10^{-2}	[37]
	W (160.00)	W/Mo (2.00)	-	-	-	-	-	[35]
	$MoSi_2$-SiC (60.00)	MO_2C (25.00)	500 °C, 1492.00 h	1.00 h cycles	SiO_2, $MoO_3Mo_4O_{11}$, Mo_9O_{26} (8.00)	$MoSi_2$-SiC (80.00)	1.00×10^{-2}	[36]

3. Conclusions

During slurry sintering, due to volatilization of solvent and binder, the prepared coating has poor surface quality and high porosity. Reducing sintering temperature and prolonging sintering time can optimize coating structure and improve coating quality to a certain extent. The lower process temperature of CVD makes the preparation efficiency of the coating low and the preparation time long. However, the technology is suitable for workpieces with complex shapes and the coatings obtained have a good low temperature oxidation resistance. In contrast, plasma spraying and the hot-dip silicon method presented a high deposition efficiency due to high diffusion temperature. After 5 to 25 min of treatment, coatings several tens to several hundred microns thick can be obtained on the substrate surface. However, the plasma-spraying coatings have a high surface roughness and porosity because the spraying material is still mixed with a small quantity of residual gas and solid particles. It is worth noting that liquid phase deposition coatings have a dense and smooth surface. This is conducive to the formation of protective oxide film on the coating surface in the oxidation process. However, the structure of the coatings are relatively simple, and the oxidation resistance of the coatings needs to be further studied. In addition, the molten salt method and laser-cladding technology have also been widely applied in the preparation of oxidation protective coatings on Mo and Mo-based alloys.

14. Pan, Y. The structural, mechanical and thermodynamic properties of the orthorhombic TMAl (TM=Ti, Y, Zr and Hf) aluminides from first-principles calculations. Vacuum 2020, 181, 109742.
15. Liu, Y.; Watanabe, M.; Miyata, R.; Nakamura, J.; Yamada, J.; Kato, H.; Yoshimi, K. Microstructures and mechanical properties of TiC-particulate-reinforced Ti–Mo–Al intermetallic matrix composites. Mater. Sci. Eng. A 2020, 790, 139–523.
16. Cui, K.K.; Fu, T.; Zhang, Y.Y.; Wang, J.; Mao, H.B.; Tan, T.B. Microstructure and mechanical properties of CaAl12O19 reinforced Al2O3-Cr2O3 composites. J. Eur. Ceram. Soc. 2021, 41, 7935–7945.
17. Niu, F.X.; Wang, Y.X.; Wang, Y.Y.; Ma, L.R.; Liu, J.J.; Wang, C.G. A crack-free SiC nanowire-toughened Si-Mo-W-C coating prepared on graphite materials for enhancing the oxidation resistance. Surf. Coat. Technol. 2018, 344, 52–57.
18. Zhang, Y.Y.; Fu, T.; Cui, K.K.; Shen, P.Q.; Wang, J.; Yu, L.H.; Mao, H.B. Evolution of surface morphology, roughness and texture of tungsten disilicide coatings on tungsten substrate. Vacuum 2021, 191, 110297.
19. Jiang, C.; Mariani, R.D.; Adkins, C.A. Ab initio investigation and thermodynamic modeling of the Mo–Ti–Zr system. Materialia 2020, 10, 100–701.
20. Zhao, M.; Xu, B.Y.; Shao, Y.M.; Zhu, Y.; Wu, J.; Wu, S.S.; Yan, Y.W. Microstructure and oxidation mechanism of multiphase Mo–Ti–Si–B alloys at 800 °C. Corros. Sci. 2021, 187, 109518.
21. Zheng, X.Q.; Liu, Y. Slurry erosion–corrosion wear behavior in SiC-containing NaOH solutions of Mo2NiB2 cermets prepared by reactive sintering. Int. J. Refract. Met. Hard Mater. 2019, 78, 193–200.
22. Gao, J.S.; Liu, Z.M.; Yan, Z.Q.; He, Y. A novel slurry blending method for a uniform dispersion of carbon nanotubes in natural rubber composites. Results Phys. 2019, 15, 102–720.
23. Li, W.; Fan, J.L.; Fan, Y.; Xiao, L.R.; Cheng, H.C. MoSi2/(Mo, Ti)Si2 dual-phase composite coating for oxidation protection of molybdenum alloy. J. Alloys Compd. 2018, 740, 711–718.

24. Cai, Z.Y.; Liu, S.N.; Xiao, L.R.; Fang, Z.; Li, W.; Zhang, B. Oxidation behavior and microstructural evolution of a slurry sintered Si-Mo coating on Mo alloy at 1650 °C. Surf. Coat. Technol. 2017, 324, 182–189.
25. Chakraborty, S.P. Development of Protective Coating of MoSi2 over TZM Alloy Substrate by Slurry Coating Technique. Mater. Today Proc. 2016, 3, 3071–3076.
26. Cai, Z.Y.; Wu, Y.H.; Liu, H.Y.; Tian, G.Y.; Pu, R.; Piao, S.M.; Tang, X.Y.; Liu, S.N.; Zhao, X.J.; Xiao, L.R. Formation and oxidation resistance of a new YSZ modified silicide coating on Mo-based alloy. Mater. Des. 2018, 155, 463–474.
27. Vaunois, J.R.; Poulain, M.; Kanouté, P.; Chaboche, J.L. Development of bending tests for near shear mode interfacial toughness measurement of EB-PVD thermal barrier coatings. Eng. Fract. Mech. 2017, 171, 110–134.
28. Gupta, M.; Li, X.H.; Markocsan, N.; Kjellman, B. Design of high lifetime suspension plasma sprayed thermal barrier coatings. J. Eur. Ceram. Soc. 2020, 40, 768–779.
29. Gorr, S.M.B.; Christ, H.J.; Schliephake, D.; Heilmaier, M. Oxidation mechanisms of lanthanum-alloyed Mo–Si–B. Corros. Sci. 2014, 88, 360–371.
30. Zhang, Y.; Pint, B.A.; Cooley, K.M.; Haynes, J.A. Effect of nitrogen on the formation and oxidation behavior of iron aluminide coatings. Surf. Coatings Technol. 2005, 200, 1231–1235.
31. Pochet, L.F.; Howard, P.; Safaie, S. Practical aspects of deposition of CVD SiC and boron silicon carbide onto high temperature composites. Surf. Coat. Technol. 1996, 86-87, 135–141.
32. Nyutu, E.K.; Kmetz, M.A.; Suib, S.L. Formation of MoSi2–SiO2 coatings on molybdenum substrates by CVD/MOCVD. Surf. Coat. Technol. 2006, 200, 3980–3986.
33. Yoon, J.K.; Kim, G.H.; Han, J.H.; Shon, I.J.; Doh, J.M.; Hong, K.T. Low-temperature cyclic oxidation behavior of MoSi2/Si3N4 nanocomposite coating formed on Mo substrate at 773 K. Surf. Coat. Technol. 2005, 200, 2537–2546.
34. Huang, X.X.; Sun, S.C.; Lu, S.D.; Li, K.H.; Tu, G.F.; Song, J.X. Synthesis and characterization of oxidation-resistant TiB2 coating on molybdenum substrate by chemical vapor deposition. Mater. Lett. 2018, 228, 53–56.
35. Du, J.H.; Li, Z.X.; Liu, G.J.; Zhou, H.; Huang, C.L. Surface characterization of CVD tungsten coating on molybdenum substrate. Surf. Coat. Technol. 2005, 198, 169–172.
36. Yoon, J.K.; Lee, K.H.; Kim, G.H.; Han, J.H.; Doh, J.M.; Hong, K.T. Low-Temperature Cyclic Oxidation Behavior of MoSi2/SiC Nanocomposite Coating Formed on Mo Substrate. Mater. Trans. 2004, 45, 2435–2442.
37. Huang, X.X.; Sun, S.C.; Tu, G.F. Investigation of mechanical properties and oxidation resistance of CVD TiB2 ceramic coating on molybdenum. J. Mater. Res. Technol. 2020, 9, 282–290.